JM3 Journal of Micro/Nanopatterning, Materials, and Metrology

RESEARCH PAPER

Sensitivity and contrast of indium nitrate hydrate resist evaluated by low-energy electron beam and extreme ultraviolet exposure

Marisol Valdez,[a] **Alexandra Joshi-Imre**,[b] **Benius J. Dunn**,[c] **Mariana Herrera Lara**,[c] **and Julia W. P. Hsu**[a,c,*]

[a]The University of Texas at Dallas, Department of Chemistry and Biochemistry, Richardson, Texas, United States

[b]The University of Texas at Dallas, Office of Research and Innovation, Richardson, Texas, United States

[c]The University of Texas at Dallas, Department of Materials Science and Engineering, Richardson, Texas, United States

ABSTRACT. We evaluate the sensitivity and contrast of indium nitrate resists by analyzing dose curves collected using electron beam lithography (EBL) and extreme ultraviolet (EUV) exposure. Three electron beam energies are tested: 100 eV, 2 keV, and 10 keV, with the dose calibrated via Faraday cup measurements. Atomic force microscopy measures the remaining resist height after EBL exposure and development for each dose. Multiple dose curves are collected at 100 eV to obtain an average contrast of 2.2 ± 0.7 and a sensitivity of 210 ± 100 $\mu C/cm^2$. Benchmarking against an organotin-cluster resist (contrast of 0.9 and a sensitivity of 210 $\mu C/cm^2$) shows that indium nitrate exhibits comparable sensitivity and contrast. A post-exposure bake (PEB) condition of 90°C for 1 min produces a noticeable leftward shift in the dose curve, corresponding to increased sensitivity. In addition, flood gun EUV exposure demonstrates a solubility switch with a sensitivity of 21 mJ/cm^2 and a remaining resist thickness of 14 nm without PEB, comparable to or better than tin-based resists. The combination of high sensitivity, good contrast, and EUV response highlights indium nitrate as a strong candidate for next-generation EUV lithography.

Keywords: inorganic extreme ultraviolet resist; electron beam lithography; indium nitrate hydrate; negative tone resist; sensitivity; contrast

Paper 24087G received Nov. 8, 2024; revised Dec. 23, 2024; accepted Jan. 8, 2025; published Jan. 28, 2025.

1 Introduction

Extreme ultraviolet (EUV) lithography is among the most advanced optical lithography techniques. It can achieve sub-10-nm resolution and support high-throughput manufacturing processes.[1,2] A major challenge in EUV lithography is identifying a resist that offers high sensitivity and resolution while meeting stringent line-edge roughness requirements. Chemically amplified resists, widely used in deep ultraviolet lithography, have underperformed in EUV applications—among other things—because they predominantly contain carbon, which has a smaller EUV absorption cross-section than metals.[3]

Inorganic metal-oxide-based resists have emerged as promising candidates for EUV lithography.[3,4] Metal elements, particularly those with filled $4d$ orbitals, exhibit large EUV cross-sections, due to the interaction of d electrons with EUV photons.[5] The most advanced

*Address all correspondence to Julia W. P. Hsu, jwhsu@utdallas.edu

commercially available inorganic EUV resists are organotin clusters commonly referenced as SnOxo. They feature organic ligands that form a cage around tin atoms, chosen for their large EUV absorption cross-section.[6,7] Upon development, SnOxo resists exhibit negative tone characteristics, where the exposed regions remain and the unexposed areas are removed.[6,7] Outside of tin-based systems, recently, there have been some efforts toward metal-containing EUV resists, including Pd/Pt organometallic resists that contain ligand complexes[8] and infiltrating trimethylindium into a conventional organic resist,[9] both still include a large organic component.

Indium, such as tin, possesses a high EUV absorption cross-section, and the nitrate ligand contains no carbon, reducing the residual carbon content in the resist.[3] We evaluate the potential of indium nitrate hydrate films as EUV resists by measuring their sensitivity and contrast from dose curves collected using electron beam lithography (EBL) and then EUV exposure. Three electron beam (e-beam) energies are tested in EBL: 100 eV, 2 keV, and 10 keV, with the dose calibrated via Faraday cup measurements. Atomic force microscopy (AFM) measures the remaining resist height after exposure and development for each dose. We further collected statistics on sample-to-sample variation by exposing indium nitrate resists at 100 eV to obtain averages and standard deviations on these properties. We also evaluate the indium nitrates' performance by benchmarking the industry standard SnOxo. We perform a post-exposure bake (PEB) study to determine the change in sensitivity. Lastly, we expose our indium nitrate sample to EUV radiation. Our results show that indium nitrate is a potential high-sensitivity EUV lithography resist.

2 Material and Methods

2.1 Fabrication of Indium Nitrate Hydrate Resist

Indium nitrate hydrate $(\mathrm{In(NO_3)_3 \cdot \mathit{x}H_2O})$ was purchased from Thermo Fisher Scientific (No. 010708), whereas the remaining chemicals were purchased from Sigma-Aldrich: 2-methoxyethanol (2-MOE), 2,4-pentanedione (AcAc), and ammonium hydroxide ($\mathrm{NH_4OH}$). The indium nitrate hydrate was stored in a $\mathrm{N_2}$ purge box, and the rest were stored at ambient environment.

The resist solution was prepared by dissolving 0.1 M of indium nitrate hydrate in 2-MOE for 24 h. Subsequently, 0.1 M of AcAc and 0.17 M of $\mathrm{NH_4OH}$ were added to the solution and stirred for 18 h at room temperature.[10] This formulation is a combustion sol–gel approach in which AcAc is the fuel and nitrate acts as the oxidizer, reducing thermal conversion temperature.[11] The solution was filtered through a 0.22-μm Polytetrafluoroethylene syringe filter before application.

Double-sided polished Si (100) wafers were cut to a 3.8×1.5 cm^2 sample size. The Si samples were scrubbed with cotton swabs using liquid detergent, acetone, isopropanol, and deionized water and then subjected to a 20-min treatment in an ultraviolet ozone system (BioForce Nanoscience, Virginia Beach, Virginia, United States).

The indium nitrate hydrate film was then spin-coated onto the Si sample at 3000 rpm for 30 s. Immediately after spin coating, the film underwent a post-application bake (PAB) on a hot plate at 90°C for 2 min and ellipsometry measured the thickness at 24.7 ± 0.1 nm.

2.2 EBL and EUV Exposure

The EBL procedure utilizes a Raith 150 Two e-beam lithography tool. The beam for the EBL tool is Gaussian, with a beam size in the order of 10 nm. The indium nitrate resist was exposed to e-beam at different doses in a pattern of fifteen 5×5 μm squares. For these experiments, the step size was 10 nm. Indium nitrate was exposed to 100-eV, 2-keV, and 10-keV electrons. The beam current for the eight runs of 100-eV experiments varied from 9 to 10.7 pA. The beam currents for 2 keV and 10 keV were 10.4 and 16.7 pA, respectively.

The EUV dose curve was performed using a flood-exposure Xe source (Energetiq, EQ10, Wilmington, Massachusetts, United States) and a 200-nm Zr filter with mesh support to isolate the 13.5-nm photons. The dose exposure range is from 0 to 50 mJ/cm^2, and each dose was applied to 12 spots on the wafer. During exposure, the background pressure of the vacuum chamber was 10^{-3} to 10^{-5} torr.

2.3 Resist Development

After exposure, all samples were developed using a weak acid solution consisting of a 15:5:1 ratio of methanol:deionized water:acetic acid. The EBL-exposed samples, which were small, were submerged in the developer for 5 s and immediately rinsed with deionized water. The EBL-exposed SnOxo resist was developed for 5 s using Propylene glycol monomethyl ether acetate. The EUV-exposed samples, which were 6-in. wafers, were developed using spin coating: the weak acid developer was left on the wafer for 15 s before spinning at 1500 rpm for 30 s.

2.4 Characterization

Ellipsometry measurements of film thickness after PAB were carried out using a J.A. Woollam M-2000DI spectroscopic ellipsometer, and analysis was performed using the CompleteEASE software. Measurements were performed over a wavelength range of 190 to 1690 nm at incident angles of 55, 65, and 75 deg. Film thickness was determined using a B-spline model constructed from an initial Cauchy model fit of the transparent region of the film in the visible spectrum and with enforced Kramers–Kronig consistency for optical constants.

After development, EBL-exposed samples were examined using an optical microscope (Leica DM2500 M) equipped with a DFC450 camera. The thicknesses of the remaining films were measured using AFM (Asylum Research MFP-3D). The thicknesses of the EUV-exposed regions were measured using a spectroscopic ellipsometer (Woollam, M-2000X) and fitted using a Cauchy model.

3 Results and Discussion

3.1 Resist Properties Obtained from EBL Dose Curves

EBL experiments were performed to collect dose curves at 100 eV, which enabled us to determine the sensitivity and contrast of the indium nitrate hydrate resist. Indium nitrate films were exposed at 15 doses, ranging from 8000 to 10 $\mu C/cm^2$ [Fig. 1(a)]. Figure 1(a) shows that 13 squares are visible; the lowest dose that triggered some solubility switch is 40 $\mu C/cm^2$. To analyze the remaining resist thickness at each dose and construct a dose curve, we perform AFM imaging on each square; an example is shown in Fig. 1(b). The bump features in the resist are clusters of small crystals of indium nitrate hydrate salt.[10] The remaining resist thickness is calculated from the height histogram for each AFM image [Fig. 1(c)]. Gaussian curve fitting is used to analyze the wafer height distribution (the peak at the lower height values) and the resist height distribution (the peak at the higher height values). This fitting produces the mean values (height at the peak maximum) and standard deviations (related to peak width). The thickness of the resist is the mean of the resist height minus that of the wafer height, and the standard deviation is computed using quadrature.

To construct a dose curve from these results, the height of each square is divided by the maximum thickness t_0, which is calculated by averaging the thicknesses measured for all doses above 400 $\mu C/cm^2$. The normalized resist thickness $\frac{t}{t_0}$ is plotted as a function of dose (D) on a logarithmic scale [Fig. 1(d)]. These data are fit to a logistic curve of the form:

$$\frac{t}{t_0} = \frac{1}{1 + 10^{k \cdot \log_{10} \frac{D_{50}}{D}}}, \tag{1}$$

where D_{50} is the dose at which the resist retains half of t_0 and k is a constant. A tangent line is drawn on the logarithmic plot at D_{50}, where the slope of the fitted curve is at its maximum [dashed line in Fig. 1(d)]. The intercept of this line with a normalized thickness of 0 occurs at D_0, the dose below which the exposed resist is completely removed during development. The intercept between this line and the normalized resist thickness of 1.0 is D_{100}, representing the minimum dose where the resist retains its maximum thickness. The sensitivity for a resist is D_{100}, and the contrast γ is calculated using[12,13]

$$\gamma = \frac{1}{\log_{10}\left(\frac{D_{100}}{D_0}\right)}. \tag{2}$$

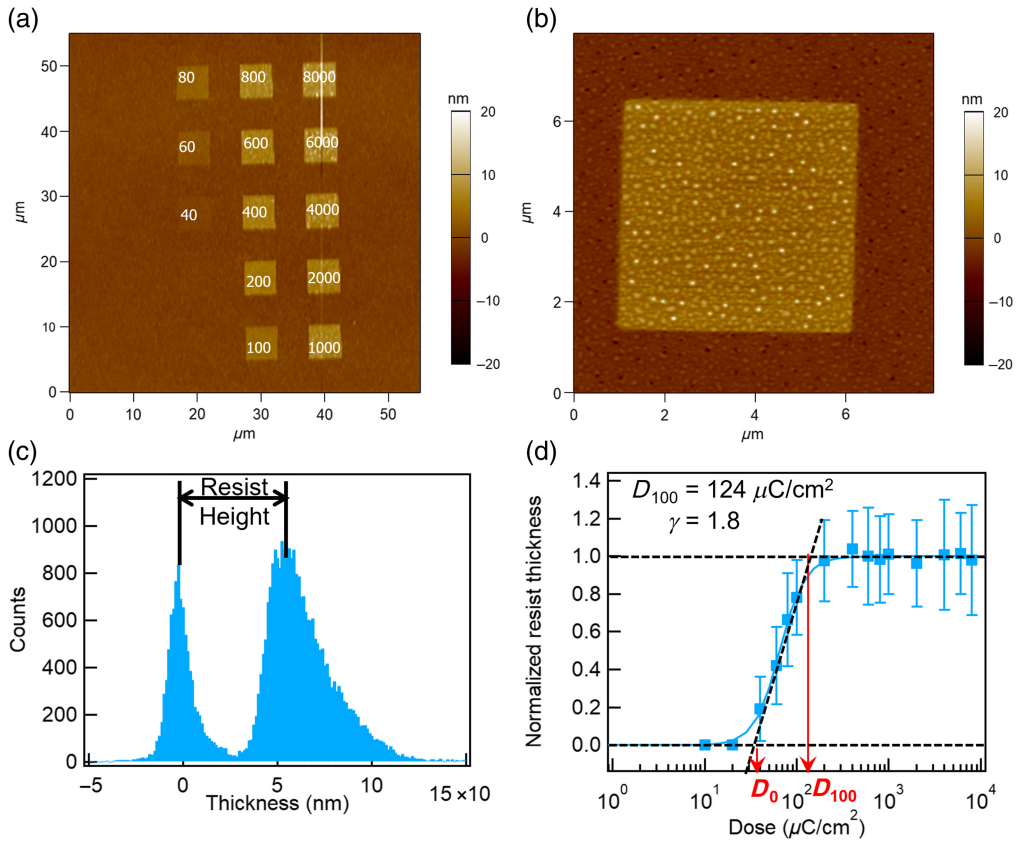

Fig. 1 (a) AFM image of an indium nitrate hydrate resist patterned by EBL at 100 eV with 15 doses (numbers in the squares, unit $\mu C/cm^2$). (b) Zoomed-in AFM image of a 5×5 μm square exposed to 8000 $\mu C/cm^2$. (c) Height histogram of the AFM image shown in panel (b). (d) Normalized resist thickness versus dose from 8000 to 10 $\mu C/cm^2$. Solid curve is the fit to Eq. (1). Dashed black line indicates the largest slope of the fitted curve.

We then performed the 100-eV EBL dose curve experiments as in Fig. 1 on multiple indium nitrate hydrate samples to examine sample-to-sample variation (Fig. 2). Each experiment was performed on a different date or the same day using different samples. Table 1 summarizes the results for the eight runs and the average contrast and sensitivity values. The contrast for indium nitrate at 100 eV EBL exposures ranges from 1.5 to 3.4, whereas the sensitivity varies between 124 and 419 $\mu C/cm^2$. The average contrast is 2.2 ± 0.7, and the average sensitivity is 210 ± 100 $\mu C/cm^2$. Notably, four patterns were made in the 121523 run (labeled 121523-1,

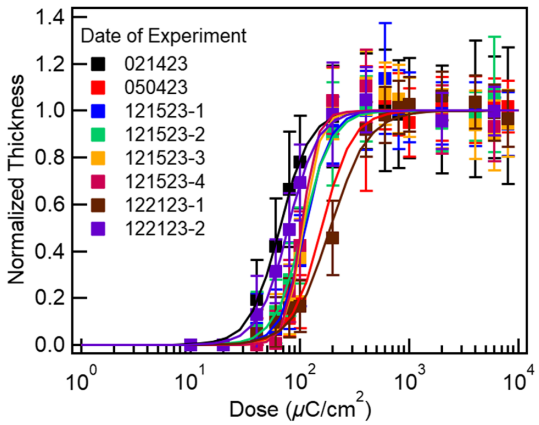

Fig. 2 Eight dose curves for indium nitrate hydrate with 100-eV EBL exposure. Solid curves are fits to Eq. (1).

Table 1 Summary of contrast, sensitivity, and thickness from eight 100-eV EBL dose curves for indium nitrate.

Date of experiment	Contrast γ	Sensitivity D_{100} (μC/cm^2)	Thickness t_0 (nm)
021423	1.8	124	5.8
050423	1.8	304	12
121523-1	2.2	189	12
121523-2	1.9	197	13
121523-3	3.1	156	10
121523-4	3.4	145	10
122123-1	1.5	419	9.1
122123-2	1.8	146	11
Average	2.2 ± 0.7	210 ± 100	10 ± 2.2

2, 3, and 4). Variations in sensitivity and contrast are observed among these samples. Table 1 shows that t_0 for each run ranges from 5.8 to 13 nm, and the average thickness for all eight runs is 10 ± 2.2 nm. These values can differ due to the subtle differences in environmental factors such as humidity, as discussed by Grayson et al.[10]

3.2 Benchmarking with SnOxo

EBL dose curve according to Fig. 1 was also collected on SnOxo to benchmark the indium nitrate resist (Fig. 3). Indium nitrate (black squares) exhibits a steeper logistic curve slope than SnOxo (red diamonds), indicating higher contrast. The indium nitrate results are from the 021423 run, which yields a contrast of 1.8 and a sensitivity of 124 μC/cm^2. The SnOxo dose curve exhibits a contrast of 0.9 and a sensitivity of 210 μC/cm^2. These two dose curves are compared because they were exposed and developed on the same day. Although the t_0 for the SnOxo resist is larger than that of the indium nitrate for run 021423 (11 versus 6 nm), it is comparable to the average of t_0 for all indium nitrate runs, 10 ± 2.2 nm (Table 1). When comparing the average contrast and sensitivity values in Table 1, the indium nitrate resist demonstrates better contrast than SnOxo, with similar sensitivity.

Previous reports on Sn-based resists show a wide variation in sensitivity under e-beam exposure, ranging from 12 to >1350 μC/cm^2.[14] The highest sensitive resist displayed a 12-μC/cm^2

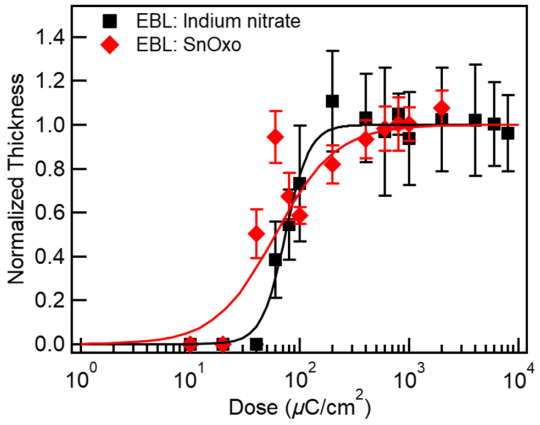

Fig. 3 100-eV EBL dose curves for indium nitrate (black squares) and SnOxo (red diamonds). The normalizing thicknesses are 6 nm for indium nitrate and 11 nm for SnOxo. Solid curves are fits to Eq. (1).

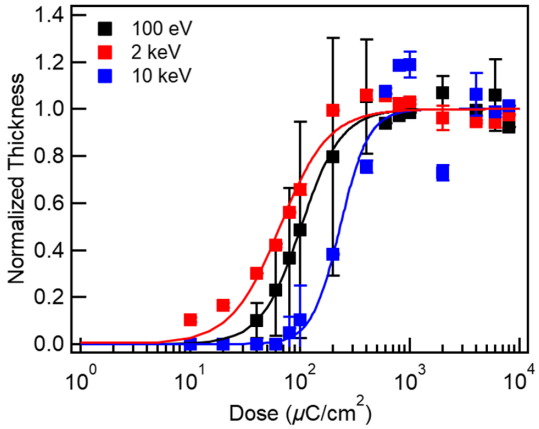

Fig. 4 Dose curves of indium nitrate resist measured at three different electron beam energies: 100 eV, 2 keV, and 10 keV. Solid curves are fits to Eq. (1).

Table 2 Contrast, sensitivity, and thickness for indium nitrate resists exposed to three electron beam energies at 100 eV, 2 keV, and 10 keV.

	Contrast γ	Sensitivity D_{100} (μC/cm^2)	Thickness t_0 (nm)
100 eV	1.4	240	10 ± 2.2
2 keV	1.1	180	9.2 ± 0.1
10 keV	1.9	420	7.6 ± 0.1

sensitivity for an organotin carboxylate resist under 2-keV e-beam exposure.[15] However, no reports were made using e-beam energies comparable to EUV photon energy as we did here.

3.3 Different E-Beam Energies

Dose curves on indium nitrate hydrate films were collected using three EBL energies: 100 eV, 2 keV, and 10 keV (Fig. 4). Table 2 summarizes the results of Fig. 4. Dose curves were averaged over two patterns made on the same sample. The maximum thickness measured was 10 nm for both 100 eV and 2 keV, whereas the 10-keV exposure produced a thickness of 8 nm. As the energy increased, there were noticeable changes in the dose curves. The contrast and sensitivity for 100 eV and 2 keV exposures are similar, as seen in Table 2. However, at lower doses, around 10 or 20 μC/cm^2, the 2-keV exposure retains a non-zero thickness, which can be explained by the larger electron penetration depth. The sample exposed to 10 keV e-beam exhibits the highest contrast value of the three energies but has the lowest sensitivity at 420 μC/cm^2. We found that 2- and 10-keV dose curves are more repeatable, whereas 100 eV is more sensitive to the details of the preparation process. We speculate that because 100-eV electrons mainly interact with the top surface of the film,[16] it may be more sensitive to surface chemistry. This observation is consistent with previous reports on other e-beam resists, which attributed the decrease in sensitivity at higher energies to fewer secondary electrons being produced per primary electron and the primary electrons having less interaction with the materials due to the larger penetration depths.[16–18] Thus, indium nitrate resists behave similarly for electron energy below 2 keV.

3.4 PEB Effects

Figure 5 compares dose curves of indium nitrate with (red squares) and without PEB (black circles). PEB was performed at 90°C for 1 min. Both samples were prepared on the same day using the same indium nitrate sol–gel precursor solution. The samples were exposed to finer dose intervals ranging from 2000 to 40 μC/cm^2. The EBL dose curves represent the average of three patterns for both No-PEB and PEB 90°C samples. The samples exhibit differences in the maximum thickness, with the No-PEB sample measuring 14 nm, whereas the PEB 90°C sample

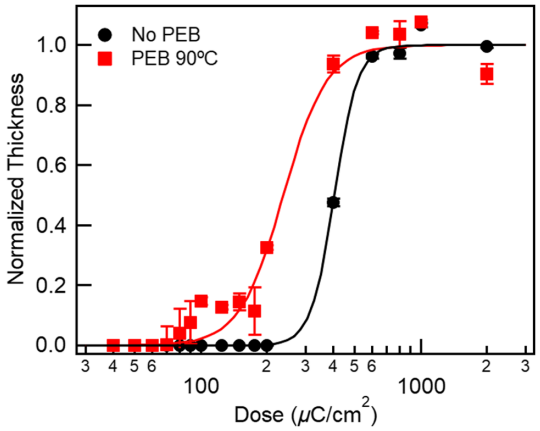

Fig. 5 100-eV EBL dose curves of indium nitrate resists that were not treated with PEB (no PEB, black circles) and with PEB (PEB 90°C, red squares). Solid curves are fits to Eq. (1).

Table 3 Contrast, sensitivity, and thickness for indium nitrate resists exposed to 100-eV electron beam and then undergoing no PEB versus PEB 90°C.

	Contrast γ	Sensitivity D_{100} (μC/cm^2)	Thickness t_0 (nm)
No PEB	4.7	513	14
PEB 90°C	2.5	375	24

retained the original thickness of 24 nm after developing with weak acid. Table 3 summarizes the sensitivity and contrast results. The no-PEB sample displayed a lower sensitivity of 535 μC/cm^2 and a sharper contrast, whereas the PEB 90°C sample demonstrated higher sensitivity, with a value of 375 μC/cm^2. The PEB 90°C treatment resulted in the resist maintaining its original thickness before exposure, and at lower doses, it showed a non-zero thickness compared with the sample without PEB.

3.5 EUV Characterization

We also performed dose curve measurements on indium nitrate using a flood gun EUV source at Intel (Fig. 6). The film was analyzed at various stages: before exposure ("as-coated"), after exposure ("post-EUV"), and after development ("post-develop"). The "as-coated" data (black circles)

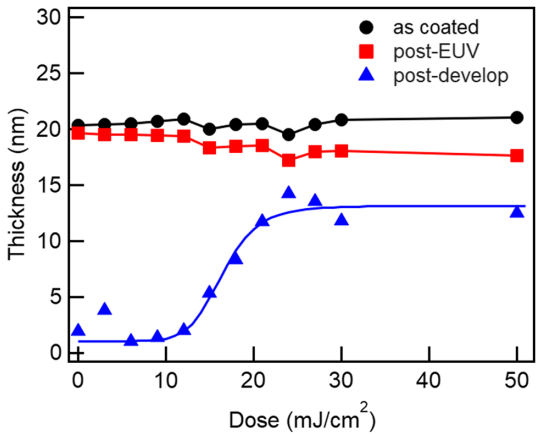

Fig. 6 Thickness versus dose for post-PAB (as-coated, black circles), before development (post-EUV, red squares), and after development (post-develop, blue triangles). The blue curve is the fit to Eq. (1).

refer to the indium nitrate resist after PAB. The "post-EUV" data (red squares) represent the indium nitrate resist after exposure to different doses. The "post-develop" data (blue triangles) show the remaining resist thicknesses after developing with unconverted resist removed. The post-EUV resist (the red squares) shows that, after exposure, there is minimal shrinkage for all doses (0 to 50 mJ/cm^2), but shrinkage increases with dose. As shown in Fig. 6, the "post-develop" film exhibits a clear solubility switch. The contrast and sensitivity are 4.7 and 21 mJ/cm^2, respectively, with a maximum resist thickness of 14 nm remaining. This result shows that the reaction happens within the resist film upon EUV exposure, but portions remain unconverted and are only removed with the developer solution. The sensitivity of 21 mJ/cm^2 for the indium nitrate resist is comparable to or even better than the reported values for the Sn-based resists, ranging from 50 to 600 mJ/cm^2.[7,19,20]

4 Conclusion

This study characterizes indium nitrate resist properties through EBL and EUV exposure. We use AFM to measure the remaining resist thicknesses of the EBL-exposed areas to form the dose curves, which are analyzed using a logistic function to determine the resist's contrast and sensitivity. For 100-eV electron beam exposure, the indium nitrate resist exhibits an average contrast of 2.2 ± 0.7 and an average sensitivity of 210 ± 100 $\mu C/cm^2$, closely matching the performance of SnOxo, which shows a contrast of 0.9 and a sensitivity of 210 $\mu C/cm^2$; 2-keV exposure produces results comparable to 100 eV, whereas 10-keV exposure produces higher contrast but lower sensitivity. PEB shifts the dose curve leftward with a higher sensitivity but lower contrast; it also maintains the precursor resist's thickness. Under EUV exposure, the resist showed a sensitivity of 21 mJ/cm^2 with a contrast of 4.7, comparable or better than Sn-based inorganic resists. These results suggest that indium nitrate is a strong candidate as an advanced metal-oxide resist for EUV lithography.

Disclosures

The authors declare that there are no financial interests, commercial affiliations, or other potential conflicts of interest that could have influenced the objectivity of this research or the writing of this paper.

Code and Data Availability

The code for the resist height and dose curve analysis are provided on GitHub. The GitHub repository can be found in the bullet point below. All scripts are written for the MATLAB software.

- The data presented in this article are publicly available on GitHub at https://github.com/UTD-Hsu-Lab/Dose-Curve-analysis.
- The archived version of the code described in this paper can be freely accessed through GitHub at https://github.com/UTD-Hsu-Lab/Dose-Curve-analysis.

Acknowledgments

We thank TEL for providing the SnOxo-coated wafer for the benchmarking study, J. Grayson for her contribution during the initial phase of the work, and F. Bard and J. M. Blackwell from Intel Corporation's Technology Research group for performing the EUV measurement. ChatGPT 4.0 was used to clean up this paper's language and grammar. The earlier version of these results was previously published as an SPIE Proceedings paper in Ref. 21. This research is supported by the Semiconductor Research Cooperation through the Nanomanufacturing Materials and Processes Program (Grant No. 3082). J. W. P. Hsu acknowledges the support of the Texas Instruments Distinguished Chair in Nanoelectronics.

References

1. J. Van Schoot et al., "High-NA EUV lithography exposure tool: program progress," *Proc. SPIE* **11323**, 1132307 (2020).

2. K. Ronse, "High NA EUV patterning ecosystem readiness to continue the logic scaling roadmap," *Proc. SPIE* **13273**, 1327304 (2024).
3. C. Luo et al., "Review of recent advances in inorganic photoresists," *RSC Adv.* **10**(14), 8385–8395 (2020).
4. X. Wang et al., "Progress in EUV resists towards high-NA EUV lithography," *Proc. SPIE* **10957**, 109570A (2019).
5. R. Fallica et al., "Absorption coefficient of metal-containing photoresists in the extreme ultraviolet," *J. Micro/Nanolith. MEMS MOEMS* **17**(2), 023505 (2018).
6. B. Cardineau et al., "Photolithographic properties of tin-oxo clusters using extreme ultraviolet light (13.5 nm)," *Microelectron. Eng.* **127**, 44–50 (2014).
7. J. Haitjema et al., "Extreme ultraviolet patterning of tin-oxo cages," *J. Micro/Nanolith. MEMS MOEMS* **16**(3), 033510 (2017).
8. M. Sortland et al., "Platinum and palladium oxalates: positive-tone extreme ultraviolet resists," *J. Micro/Nanolith. MEMS MOEMS* **14**(4), 043511 (2015).
9. A. Subramanian et al., "Vapor-phase infiltrated organic–inorganic positive-tone hybrid photoresist for extreme UV lithography," *Adv. Mater. Interfaces* **10**(28), 2300420 (2023).
10. J. L. Grayson et al., "Indium nitrate hydrate films as potential EUV resists: film formation, characterization, and solubility switch assessment using a 92-eV electron beam," *J. Micro/Nanopattern. Mater. Metrol.* **23**(1), 014601 (2024).
11. M. G. Kim et al., "Low-temperature fabrication of high-performance metal oxide thin-film electronics via combustion processing," *Nat. Mater.* **10**(5), 382–388 (2011).
12. Y. Wang et al., "A single-component molecular glass resist based on tetraphenylsilane derivatives for electron beam lithography," *ACS Omega* **8**(13), 12173–12182 (2023).
13. J. Shi et al., "Molecular layer deposition of a hafnium-based hybrid thin film as an electron beam resist," *ACS Appl. Mater. Interfaces* **14**(23), 27140–27148 (2022).
14. S. Woo et al., "Layer-ordered organooxotin clusters for extreme-ultraviolet photolithography," *ACS Appl. Mater. Interfaces* **16**(30), 39580–39591 (2024).
15. M. C. Sharps et al., "Organotin carboxylate reagents for nanopatterning: chemical transformations during direct-write electron beam processes," *Chem. Mater.* **31**(13), 4840–4850 (2019).
16. H. Shinotsuka et al., "Calculations of electron inelastic mean free paths. X. Data for 41 elemental solids over the 50 eV to 200 keV range with the relativistic full Penn algorithm," *Surf. Interface Anal.* **47**(9), 871–888 (2015).
17. M. A. Mohammad et al., "Fundamentals of electron beam exposure and development," in *Nanofabrication: Techniques and Principles*, M. Stepanova and S. Dew, Eds., pp. 11–41, Springer Vienna, Vienna (2012).
18. S. M. Lewis et al., "Tuning the performance of negative tone electron beam resists for the next generation lithography," *Adv. Funct. Mater.* **32**(32), 2202710 (2022).
19. J.-R. Wu et al., "Novel hexameric tin carboxylate clusters as efficient negative-tone EUV photoresists: high resolution with well-defined patterns under low energy doses," *Nanoscale Adv.* **5**(11), 3033–3043 (2023).
20. R. Del Re et al., "Low-LER tin carboxylate photoresists using EUV," *Proc. SPIE* **9422**, 942221 (2015).
21. M. Valdez et al., "Indium nitrate hydrate resist characteristics evaluated by low-energy electron beam exposure," *Proc. SPIE* **12957**, 129570Q (2024).

Julia W. P. Hsu is a professor of materials science and engineering at the University of Texas at Dallas and holds the Texas Instruments Distinguished Chair in Nanoelectronics. She is a fellow of the American Physical Society, American Association for the Advancement of Science, Materials Research Society, and Institute of Physics. Her current research activities include novel materials and processing techniques for organic and perovskite solar cells, flexible electronics, and inorganic EUV resists. She is a member of SPIE.

Biographies of the other authors are not available.